Distributed feedback photonic crystal fibre (DFB-PCF) laser

Nathaniel Groothoff
Optical Fibre Technology Centre - University of Sydney
206 National Innovation Centre, Australian Technology Park, Eveleigh NSW 1430 Australia.
School of Physics - University of Sydney, NSW 2006 Australia.

John Canning, Tom Ryan, Katja Lyytikainen
Optical Fibre Technology Centre - University of Sydney
206 National Innovation Centre, Australian Technology Park, Eveleigh NSW 1430 Australia.
j.canning@oftc.usyd.edu.au

Hugh Inglis
Redfern Optical Components Pty. Ltd.
National Innovation Centre, Australian Technology Park, Eveleigh, Sydney NSW 1430 Australia

Abstract: A distributed feedback laser is fabricated in Er^{3+}-doped photonic crystal fibre. Preferential single-mode lasing is obtained with no special consideration of polarisation issues. The results demonstrate practical implementation of a multi-photon writing process for complex structures in these optical fibres. No hydrogen loading and no germanium are involved.
©2005 Optical Society of America

OCIS codes: (160.4670) Optical materials; (230.1150) All-optical devices (999.9999) Optical waveguides; (999.9999) Fresnel fibres; (999.9999) Scattering; (999.9999) Photonic crystal waveguides; (999.999) air-silica structured waveguides; (999.9999) fibre lasers; (999.999) lasers; (999.999) distributed Bragg reflector, (999.999) multiphoton absorption; (999.999) bandgap; (999.999) zone

References and links

1. J. Canning, N. Groothoff, E. Buckley, T. Ryan, K. Lyytikainen and J. Digweed, "All-fibre photonic crystal distributed Bragg reflector (PC-DBR) fibre laser" Opt. Express **11**, 1995-2000 (2003)
2. J. Albert, M. Fokine, and W. Margulis, "Grating formation in pure silica-core fibers," Opt. Lett., **27**, 809-811 (2002)
3. N. Groothoff, J. Canning, E. Buckley, K. Lyttikainen and J. Zagari, "Bragg gratings in air-silica structured fibers," Opt. Lett. **28**, 233-235 (2003)
4. C. Martelli, J. Canning, N. Groothoff and K. Lyytikainen, "Bragg Gratings in Photonic Crystal Fibres: Strain and Temperature Characterisation," Accepted to Opt. Lett. (2005)
5. J. Canning, "Diffraction-Free Mode Generation and Propagation in Optical Waveguides," Opt. Commun. **207,** 35-39 (2002)
6. J. Canning, E. Buckley, K. Lyytikainen, "Propagation in air by field superposition of scattered light within a Fresnel fibre," Opt. Lett. **28**, 230-2332 (2003)
7. J. Canning, E. Buckley, K. Lyytikainen, "All-Fibre Phase-Aperture Zone Plate Fresnel Lenses," Electron. Lett., **39**, 311-312 (2003)
8. J. Canning, "Fibre lasers and related technologies," Accepted to Opt. & Las. In Eng. (2005)
9. W. Primak, E. Edwards, "Radiation induced dilations in vitreous silica," Phys. Rev. **128**, 2580–2588 (1962)
10. C. Fiori and R. A. B. Devine, "Evidence of a wide continuum of polymorphs in α-SiO_2," Phys. Rev. **B 33**, 2972–2974 (1986)
11. A. Wootten, B. Thomas, P. Harrowell, "Radiation-induced densification in amorphous silica: A computer simulation study," J. Chem. Phys., **115**, 3336-3341 (2001)
12. J. Canning, M. G. Sceats, "π-phase-shifted periodic distributed structures in germanosilicate fibre by uv post-processing," Electron. Lett. **30**, 1344-1345 (1994)

#6785 - $15.00 US Received 8 March 2005; revised 30 March 2005; accepted 1 April 2005
(C) 2005 OSA

1. Introduction

In previous work we demonstrated the first grating based photonic crystal fibre laser where the gratings were inscribed directly into the air-structured waveguide [1]. The importance of combining recent work writing passive gratings using a two-photon process [2] in pure silica structures with air holes [3] that can be filled for specific custom functionality was emphasised. For example, in sensing and diagnostic applications the material or species to be detected can enter the airholes to maximise overlap with the resonant structures. However, in addition the air structure in these fibres can be tailored to have unique macro properties that can be measured by gratings, including strain optic responses distinct to that of conventional fibre [4]. At its simplest, this permits a method to circumvent the challenge involved in separating thermal and strain responses from a Bragg grating in many sensor applications. Thus real near-field engineering within the waveguide using such "meta-materials" is possible, particularly as the air holes become small compared to the wavelength of light. Combined with far-field control by a new class of Fresnel fibres that implicitly recognise the zone plates of the waveguide [5-7], where the simplest design is equivalent to a chirped Bragg fibre [5], total optical field and material engineering of silica and other materials is increasingly possible. It is evident that in combination with active gratings, where the resonances are enhanced by the presence of gain, further significant improvement of all these features can be achieved. Still further, the opportunity of combining the 1-D features of a Bragg grating structure with a 2-D surrounding structure will eventually allow refined engineering of radiation emission and other characteristics of active photonic bandgap devices. In pursuing this line of work, we report the first distributed feedback photonic crystal fibre (DFB-PCF) laser. In master oscillator power amplifier configurations, (either double-clad, triple clad or air-clad power amplifiers), DFB fibre lasers can deliver watts of power before consideration of nonlinear Brillouin scattering becomes critical, opening up additional high power applications [8]. The results reported here using multi-photon excitation of the silica band edge (in our case with two photons at 193nm) could be directly applied to grating and DFB laser fabrication within all these fibres. The multiphoton approach builds on decades of research understanding radiation-induced compaction and dilation of glass networks when excited well below the UV band edge of the network [9-11].

2. Rare-earth doped photonic crystal fibre fabrication

The photonic crystal fibre is manufactured from a preform consisting of an array of capillaries drawn down to suitable dimensions. The light-guiding core region itself is fabricated by etching a preform produced by modified chemical vapour deposition (MCVD) such that a solid capillary ~2mm wide containing the $Er^{3+}$is obtained. The additional incorporation of aluminium reduces clustering, allows higher concentrations and promotes greater homogeneity of the rare earth. However, it does raise the local index slightly higher than the surrounding silica region defined by the capillaries after stacking and drawing [1]. Optical fibres of varying diameters were then drawn from the preform. The photonic crystal fibre (PCF) diameter used in this study was 100μm, chosen because it has the lowest confinement and coupling loss with standard single-mode telecommunications fibre at 980nm. A total concentration of ~0.12wt% of Er_2O_3 is estimated from a measured absorption of 72dB/m at 1530nm. The small signal gain coefficient is measured to be around 0.32dB/cm at 1532nm – more details can be found in [1]. Assuming an ideal lossless resonant cavity with sufficient Q, a DFB laser as short as 3cm is theoretically possible in this fibre.

3. Resonant phase shifted cavity

The 193nm output of an exciplex ArF laser (λ=193nm, pulse-to-pulse fluctuation <2%, pulse width=15ns) was focussed such that the intensity overlapping across the fibre core defined by the first ring is high enough to allow excitation of the band edge by two-photon absorption but low enough to prevent damage during writing. Although damage gratings written by multi-photon excitation occur quite easily, and there is an associated improvement in thermal

#6785 - $15.00 US Received 8 March 2005; revised 30 March 2005; accepted 1 April 2005
(C) 2005 OSA

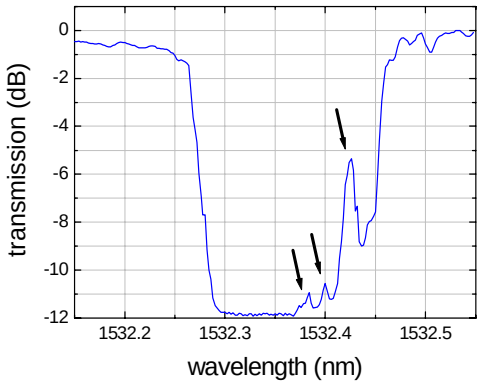

Fig. 1. Transmission profile of the phase shifted structure inscribed within an Er^{3+} doped photonic crystal fibre.

stability analogous to type II damage gratings, the induced scattering losses can substantially reduce the cavity Q of the laser. We therefore operate below this threshold such that densification, and possible dilation, is the mechanism underpinning the index change [8-10]. The intensity used was well above that required for 1-photon grating writing, a process we found to be inefficient in this fibre without hydrogen loading. Further, we avoided all grating-cladding resonances by using a two-photon approach [3].

Writing two gratings with a small gap inbetween produced the phase-shifted structure. We chose a DFB structure of length 10cm to ensure enough gain is present for lasing and to compensate for any losses in the real system. To achieve the intensity necessary for two-photon absorption, the laser was focused onto the fibre (pulse energy = 230mJ/cm^2).

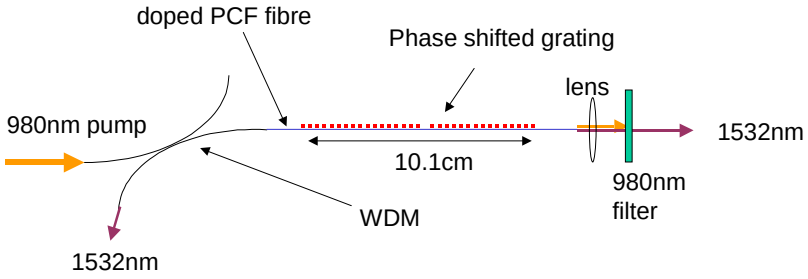

Fig. 2. Schematic of laser cavity and pumping scheme

The Rayleigh range of the lens was sufficiently long to ensure that the index change is across the entire core defined by the first ring of air holes removing unwanted core-leaky and radiation mode coupling. Each grating was 50mm long, with a 1mm gap between them, achieved by scanning at a constant velocity along the fibre with a total fluence of 27kJ/cm^2 and 26kJ/cm^2 respectively. A lower fluence for the second was attributed to a decrease in laser power during writing. This necessitated additional post processing to fine tune the phase shift into the band gap of the grating [12]. A computer controlled tuneable laser source (resolution 1pm) and power meter were used to monitor the grating growth and phase shift notch spectral position. Standard telecommunications fibre was spliced onto each fibre end with most of the insertion loss accounted for by the effective V-parameter mismatch between fibres. Although optimised in terms of fundamental mode coupling with telecommunications fibre, this fibre supports a higher order mode [1], and in combination with the absorption and splice loss, a practical signal-to-noise floor of ~12 dB is obtained. Figure 1 shows the final transmission spectra. Both the grating bandgap and the main notch are broad for a 10cm grating indicating a small amount of chirp attributed to the intensity variation during writing – the two-photon process is very sensitive to small power fluctuations, a situation that is compounded substantially in higher exponent multiphoton exposure processes whilst translating the beam

#6785 - $15.00 US
Received 8 March 2005; revised 30 March 2005; accepted 1 April 2005
(C) 2005 OSA

(or fibre). The grating strength is estimated, through numerical simulation, to be around 15-25dB, depending on the presence of chirp. As well as broadening the notches and reducing the cavity Q, the chirp limits the placement of the resonant notch to one side of the spectrum despite continued processing (cumulative fluence used was 192kJ/cm^2). The two small peaks closer to the centre may be attributed to polarisation splitting and the presence of another mode defined by the step index created by the aluminium and Er^{3+}. By having two criteria defining a fundamental mode – the step index of the doped region and the step index of the air hole region - the fundamental mode is likely to be non-degenerate and made up of two very closely spaced modes. These in turn may have distinct polarisation splitting, explaining why more than one additional notch is observed in the transmission spectra.

4. DFB-PCF laser

Figure 2 shows a schematic of the pump configuration of the laser. The cavity was pumped using a 980nm diode laser coupled through a 980/1550nm wavelength division multiplexer (WDM). The output power of the laser was measured from both ends. Pumping of the laser was carried out through spliced single-mode fibres at either end and through free-space coupling. The latter method produced slightly higher total output powers indicating that matching the fibre V-parameters is important. The output power co-propagating with the 980nm pump light, was measured using a power meter after passing through an objective lens and 980nm filter. Figure 3 displays the total power (assuming equal powers from both ends) along with the emission spectrum (figure 3 inset) measured on an optical spectrum analyser (OSA) with resolution of 50pm. The wavelength differs to that from the grating transmission spectrum because the setup used to pump the laser is different to that used to measure the transmission and hence differences in tension along the fibre are present. The power and spectrum were also obtained through the WDM for the 1550nm output counter-propagating with the pump. Similar results were estimated once losses attributed to the WDM were considered. From this data the lasing threshold is determined to be 30mW and the slope efficiency η = 12.5%. We attribute the high threshold to the likelihood that some of the pump light is coupled into a higher order mode that sees little of the gain. The grating chirp, which reduces the cavity Q and the accessible gain of the cavity, can explain the low efficiency. Further improvements can be expected with better gratings. The total power output achieved with this laser is ~5mW – no saturation level is observed indicating that complete population inversion is not occurring and more output power is feasible with increased pump power.

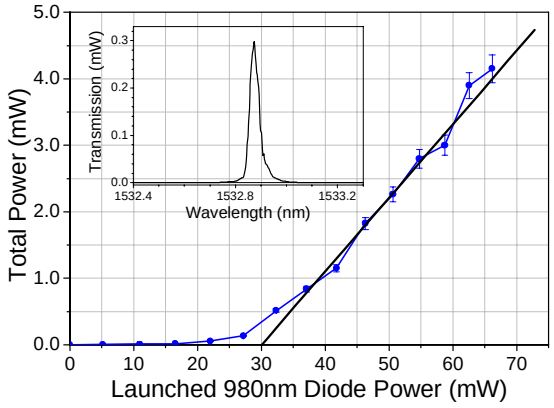

Fig. 3. Total emitted power from DFB-PCF laser. Inset: OSA spectrum of laser.

#6785 - $15.00 US Received 8 March 2005; revised 30 March 2005; accepted 1 April 2005
(C) 2005 OSA

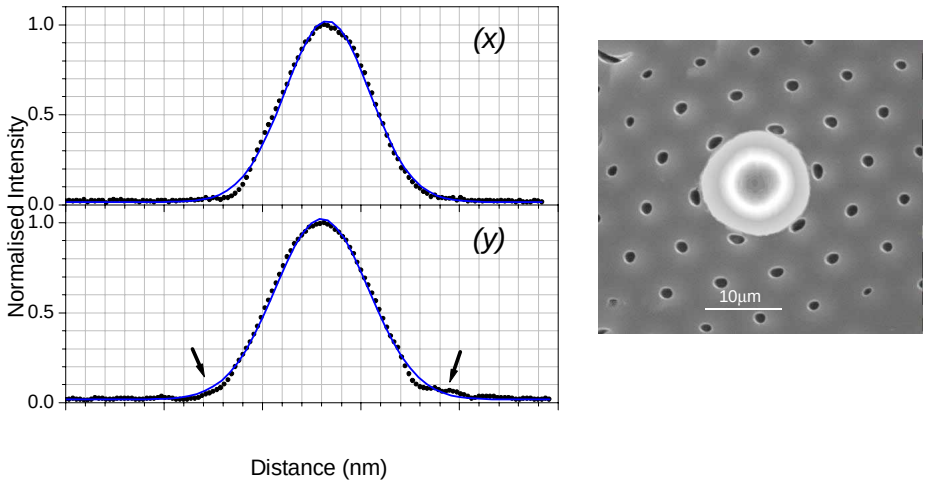

Fig. 4 (Left) *x* and *y* intensity cross-sections of laser mode profile with Gaussian fits and (Right) SEM image with near field profile of laser output. The SEM image does not line up with the orientation of the cross-sections.

Replacing the power meter with a camera enabled a near-field profile of the lasing mode in the fibre. This is superimposed on a scanning electron microscope (SEM) image of the fibre end face, shown in figure 4. Cross sectional intensity profiles of *x* and *y* directions show excellent agreement with a Gaussian fit indicating that the laser oscillates on a single transverse mode – the small "humps" of the *y* profile, as indicated by the arrows in figure 4*(y)*, show that the slice was taken partly inbetween two air-holes where circular symmetry is not present. The profile indicates that the ring of air holes determines the fundamental mode of the laser. To analyse the longitudinal mode structure, the laser was launched into a Fabry-Perot interferometer (FPI). Figure 5 shows one lasing mode is present. At times a second mode was observed to appear approximately where the two arrows designate. In a conventional DFB fibre laser this would be attributed to the second polarisation eigenstate of the cavity but we cannot rule out the possibility that lasing may also be occurring from another mode defined by the step index region created with aluminium and Er^{3+} doping. Further, occasionally with adjustment it is possible to get three lasing modes, consistent with the observed three notches in the transmission profile (figure 1). Since this laser is unpackaged, some influence of environmental noise in determining the onset of these other modes cannot be ruled out; particularly since the pump light is likely to be propagating as both fundamental and higher order modes.

To explore this further, along with FPI spectra the relative intensity noise (RIN = $\overline{P}^2_{noise} / \overline{P}^2_{signal}$) was also measured and is shown in Figure 6. Although the peak associated with the relaxation oscillations of the rare earth ions is evident, the profile has a dip at this peak indicating large fluctuations that can be explained as arising mostly from coupling between fundamental and higher order modes of the pump. It is possible that the occasional lasing of other modes (doped step index and polarisation eigenstates) may play a role but the measurements were taken when lasing was stable. If present, the independence of each lasing mode, possibly through spatial and polarisation hole burning, is not known and hence contribution of mode partition noise in the RIN spectrum may need consideration. In any case, all modes are sensitive to any pump variations between fundamental and higher order modes. Put into context, the overall RIN value of -44dB/Hz is larger than normally specified for commercial applications but may be significantly reduced with improved fibre design and

#6785 - $15.00 US Received 8 March 2005; revised 30 March 2005; accepted 1 April 2005
(C) 2005 OSA

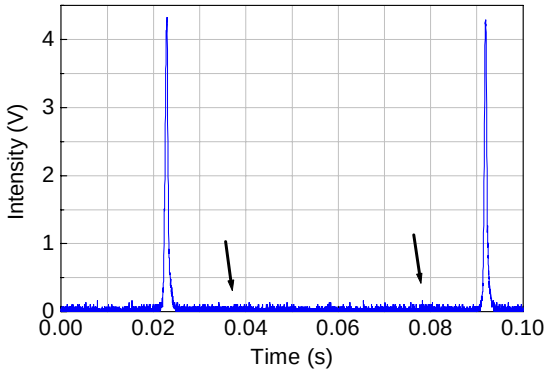

Fig. 5. FPI spectra. FSR = 1.5GHz and f = 100. Arrows depict where onset of second lasing mode can occur.

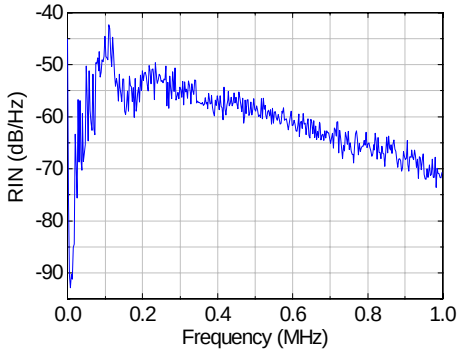

Fig. 6. Relative intensity noise (RIN) measurement for the DFB-PCF laser.

appropriate packaging, including twisting of the cavity to reduce any polarisation contributions.

5. Conclusions

The use of multi(two)-photon excitation of the band edge of silica has enabled the fabrication of the first distributed feedback laser in a photonic crystal fibre. No detrimental issues arising from air-hole structure were observed. This signifies the first practical demonstration of a multi-photon grating writing approach to inscribe a complex structure into a fibre (namely a photonic crystal fibre) by translation. Some question marks remain over the viability of higher exponent multi-photon processes targeted below the glass band edge where the practical intensity required for structural rearrangement leading to densification and dilation is close to the damage threshold. In contrast, we believe two photon grating writing intrinsically offers the potential to disrupt existing grating writing methods based on specific defect excitation introduced by dopants such as germanium. The ability to add other material in photonic crystal fibres, including alternative gain media such as dyes, or gases that enhance Raman and other nonlinear effects, significantly widens the potential advances in fibre laser technology. For example, the possibility of anti-resonant waveguide DFB lasers, where material with a higher index than glass is placed into the air holes after grating writing, also becomes feasible. In sensing applications, such as gas detection, the inclusion of media into the air holes in combination with tailored mode overlap profiles promises substantial enhancement in

#6785 - $15.00 US Received 8 March 2005; revised 30 March 2005; accepted 1 April 2005
(C) 2005 OSA

sensitivity. The exploitation of an appropriately designed lattice of air holes will in all likelihood lead to further improvements, including lower thresholds.

Acknowledgments

Mark Englund of Redfern Optical Components (ROC) Pty Ltd is thanked for permitting the use of ROC's automated characterisation equipment. Technical assistance from Goran Edvell is appreciated. This work and N. Groothoff's scholarship are funded through an Australian Research Council (ARC) Discovery Project.

#6785 - $15.00 US Received 8 March 2005; revised 30 March 2005; accepted 1 April 2005
(C) 2005 OSA